DMD Fast Forward. Published on October 5, 2020 as DOI: 10.1124/dmd.120.000145
This article has not been copyedited and formatted. The final version may differ from this version.

Anti-Ly6E-*seco*-CBI-Dimer Antibody-Drug Conjugate (ADC) That Forms Adduct with Alpha-1-microglobulin (A1M) Demonstrates Slower Systemic Antibody Clearance and Reduced Tumor Distribution in Animals

Victor Yip[1], Isabel Figueroa[1], Brandon Latifi[1], Shab Masih[1], Carl Ng[2], Doug Leipold[1], Amrita Kamath[1], and Ben-Quan Shen[1*]

[1]*Preclinical and Translational Pharmacokinetics, Genentech, South San Francisco, CA 94080, USA*

[2] *Bio-Analytical Sciences, Genentech, South San Francisco, CA 94080, USA.*

DMD Fast Forward. Published on October 5, 2020 as DOI: 10.1124/dmd.120.000145
This article has not been copyedited and formatted. The final version may differ from this version.

Running title: ADC formed adduct with A1M impacts PK and tumor distribution

[*]**Corresponding author:**

Ben-Quan Shen, M.D.

Preclinical and Translational Pharmacokinetics and Pharmacodynamics

Genentech, Inc.

1 DNA Way

South San Francisco, CA 94080;

e-mail: bqshen@gene.com;

Tel: 001-650-2258814

Number of text pages: 44

Number of Table: 2

Number of Figures: 8

Number of references: 29

Number of words in sections:

Abstract: 249

Introduction: 733

Discussion: 1497

Abbreviations: A1M, Alpha-1-microglobulin; ADC, antibody-drug conjugate; AUC_{INF}, area under the concentration–time curve extrapolated to infinity; C_{max}, maximum concentration; CBI, cyclopropabenzindol-4-one; CL, clearance; DAR, drug-to-antibody

DMD Fast Forward. Published on October 5, 2020 as DOI: 10.1124/dmd.120.000145
This article has not been copyedited and formatted. The final version may differ from this version.

ratio; DNA, deoxy nucleic acid; ELISA, enzyme-linked immunosorbent assay; gD, glycoprotein-D; IgG1, immunoglobulin G1; IV, intravenous dosing; LC/MS, liquid chromatography tandem mass spectrometry; Ly6E, Lymphocyte antigen 6 complex, locus E; mAb, monoclonal antibody; PBS, phosphate buffer saline; PK, pharmacokinetics; SEC-HPLC, size exclusion column with high performance liquid chromatography; Tab, total antibody (could include DAR2, DAR1, and DAR0 species for ADCs in this study); t_{half}, terminal half-life; V_{ss}, volume of distribution at steady state; %ID, percent of injected dose.

DMD Fast Forward. Published on October 5, 2020 as DOI: 10.1124/dmd.120.000145
This article has not been copyedited and formatted. The final version may differ from this version.

Abstract

Anti-Ly6E-*seco*-CBI dimer antibody-drug conjugate (ADC) has been reported to form an adduct with alpha-1-microglobulin (A1M) in animal plasma, but with unknown impact on ADC PK and tissue distribution. In this study, we compared the PK and tissue distribution of anti-Ly6E ADC with unconjugated anti-Ly6E mAb in rodents and monkeys. For PK studies, animals received an intravenous (IV) administration of anti-Ly6E ADC or unconjugated anti-Ly6E mAb. Plasma samples were analyzed for total antibody (Tab) levels and A1M adduct formation. PK parameters were generated from dose-normalized plasma concentrations. Tissue distribution was determined in tumor-bearing mice following a single IV dosing of radiolabeled ADC or mAb. Tissue radioactivity levels were analyzed using a gamma counter. The impact of A1M adduct formation on target cell binding was assessed in an *in-vitro* cell binding assay. The results show that ADC Tab clearance was slower than that of mAb in mice and rats, but faster than mAb in monkeys. Correspondingly, the formation of A1M adduct appeared to be faster and higher in mice followed by rats, but slowest in monkeys. While ADC trended to show an overall lower distribution to normal tissues, it had a strikingly reduced distribution to tumors in compared to mAb, likely due to A1M adduct formation interfering with target binding as demonstrated by the *in-vitro* cell binding assay. Together, these data demonstrate that anti-Ly6E ADC that forms A1M adduct had slower systemic clearance with strikingly reduced tumor distribution and highlight the importance of selecting an appropriate linker-drug for successful ADC development.

DMD Fast Forward. Published on October 5, 2020 as DOI: 10.1124/dmd.120.000145
This article has not been copyedited and formatted. The final version may differ from this version.

Significance Statement:

Anti-Ly6E ADC with *seco*-CBI dimer payload formed adduct with A1M which led to a decrease in systemic clearance, but also attenuated tumor distribution. These findings demonstrate the importance of selecting an appropriate linker-drug for ADC development, and also highlight the value of mechanistic understanding of ADC biotransformation that could provide insight into ADC molecule design, optimization and selection.

DMD Fast Forward. Published on October 5, 2020 as DOI: 10.1124/dmd.120.000145
This article has not been copyedited and formatted. The final version may differ from this version.

Introduction

Tremendous advances have been made in cancer therapeutics in the past decade. Molecule classes such as checkpoint inhibitors against programmed cell death protein 1, known as PD1, (e.g. Keytruda (anti-PD-1) and Tecentriq (anti-PDL-1) (Jin et al., 2011; Garon et al., 2019), chimeric antigen receptors-T-cell (CAR-T) (e.g. Kymriah, against CD19) (Miliotou and Papadopoulou, 2018; Seimetz et al., 2019) , and antibody-drug conjugates (ADC) (e.g. Kadcyla®, ado-trastuzumab emtansine) (Diamantis and Banerji, 2016; Abdollahpour-Alitappeh et al., 2019) have recently been marketed. These new therapeutics with improved specificity to tumor targets have dramatically improved the quality of life in the patients (Inthagard et al., 2019). However, there is still a need to better characterize the behavior of these molecules as the number of the targets being investigated is expanding. ADCs in particular, with their multiple variables such as antibody, linker, payload, and site of conjugation, have very different physical and biological properties arising from different combinations of these variables (Abdollahpour-Alitappeh et al., 2019; Birrer et al., 2019).

An ADC combines the specificity from its monoclonal antibody (mAb) and potency from its payload, where the payload by itself is usually too toxic for direct administration. By combining both antibody and payload via a linker, the antibody acts as a guide for the payload to its intended target. Numerous reports have been published showing that manipulating these variables alter the PK and efficacy of the molecules (Frigerio and Kyle, 2017; Ohri et al., 2018; Su et al., 2018). However, as both antibody and payload are

DMD Fast Forward. Published on October 5, 2020 as DOI: 10.1124/dmd.120.000145
This article has not been copyedited and formatted. The final version may differ from this version.

chemical entities, they have the potential to interact with endogenous proteins, as such resulting in biotransformation/modification of the molecules and alteration of PK and activity (Palleria et al., 2012; Sousa et al., 2008; Su et al., 2018). Though this type of biotransformation/modification is often seen in small molecule drug development, it can also occur for large molecules on a case-by-case basis. It has not been extensively reported in the development of ADC which contains both large and small molecules (Lu et al., 2013).

Lymphocyte antigen 6 complex, locus E (Ly6E) is a member of the lymphostromal cell membrane Ly6 superfamily protein. Ly6E has been shown at elevated expression level in cancer patients with breast, lung, bladder, brain, gastric, and skin cancers, and is positively correlated with poor overall survival rate (Asundi et al., 2015; AlHossiny et al., 2016). Although the exact mechanism of biological function and clinical significance of Ly6E is largely unknown, overexpression of Ly6E seems to promote cancer cell growth and metastasis. Because Ly6E is over-expressed in multiple cancer indications, it is an ideal candidate for targeted tumor delivery by an ADC. The payload of our ADC is a cyclopropabenzindol-4-one (CBI)-containing derivative, *seco*-CBI dimer (henceforth CBI-dimer) (**Figure 1**). Briefly, the phosphate pro-drugs present in the seco-CBI-dimer-containing payload are quickly removed by plasma/blood phosphates while the conjugate circulates in vivo to produce (via molecular rearrangement) the biologically active CBI-dimer entity. Following its ADC-mediated delivery to targeted cells, the released CBI-dimer payload alkylates DNA and leads to tumor apoptosis (Parrish et al., 2003). The

DMD Fast Forward. Published on October 5, 2020 as DOI: 10.1124/dmd.120.000145
This article has not been copyedited and formatted. The final version may differ from this version.

anti-Ly6E antibody and the *seco*-CBI dimer payload are linked by a maleimide moiety via a peptidomimetic, protease-cleavable linker.

Anti-Ly6E-CBI-dimer ADC was previously shown to form adducts with glutathione (GSH), and especially with alpha-1-microglobulin (A1M) in animal plasma (Su et al., 2019). The A1M alkylates to the conjugated CBI-dimer through its electrophilic moieties forming the adduct at the same site where the DNA alkylates, which slightly reduces the potency of the ADC both in-vitro and possibly in-vivo, as one of the two conjugated CBI-dimers loses its activity to cross-link with DNA (**Figure 1**). The extent of this adduct formation differs among species, for example, it is much faster in rodents than cynomolgus monkey, which could be attributed to the phosphatase activity and amount of A1M level (Su et al.; 2019). However, there is little data on whether the adduct formation would alter the PK and distribution of the anti-Ly6E ADC. Therefore, in this paper we have compared the PK between anti-Ly6E ADC (forming A1M adduct) and its unconjugated monoclonal antibody (no A1M adduct formation) in rodents and monkeys. In addition, we have further compared the tissue distribution of anti-Ly6E ADC with its unconjugated antibody in tumor-bearing mice. Here we report that the A1M adduct formation of ADC appeared to influence its PK. More importantly, the ADC-A1M adduct formation greatly attenuated tumor tissue distribution, likely by reducing target binding to tumor cells.

Materials and Methods

DMD Fast Forward. Published on October 5, 2020 as DOI: 10.1124/dmd.120.000145
This article has not been copyedited and formatted. The final version may differ from this version.

Reagents: All unconjugated and conjugated antibodies used for in vitro and in vivo PK, efficacy, and safety studies presented here were generated at Genentech Inc. (South San Francisco, CA). The unconjugated antibody (anti-Ly6E mAb) is a humanized monoclonal immunoglobulin G1 (IgG1) antibody that binds to the Ly6E human receptor. Anti-Ly6E mAb was humanized from its parental hybridoma clone that was generated by immunizing Balb/c mice with purified LY6E protein. A control non-binding antibody targeting the glycoprotein-D epitope of herpes simplex virus, anti-glycoprotein-D IgG1 antibody (anti-gD mAb), was produced and humanized at Genentech, Inc. Mouse plasma used in *in-vitro* preincubation was purchased from BioIVT (Cat# MSEPLLIHP, Westbury, NY).

ADC conjugation: The anti-Ly6E antibody drug conjugate (anti-Ly6E ADC) corresponds to anti-Ly6E mAb carrying two molecules of a cytotoxic drug (a DNA damaging agent), also referred to as payload. The payload is a *seco*-CBI dimer conjugated to the antibody via a cleavable disulfide-labile linker (**Figure 1**). The linker-drug has been described in a previous publication (as linker-drug 10) (Su et al., 2019). Anti-Ly6E ADC uses THIOMAB^{TM} antibody technology resulting in the conjugation of two drug molecules per antibody to engineered cysteine residues (Junutula et al., 2008a; Junutula et al., 2008b).

Radiolabeling: Anti-Ly6E ADC and anti-Ly6E mAb were both radiolabeled with ^{125}I (non-residualizing) or ^{111}In with 1,4,7,10-tetraazacyclododecane-N,N',N,"N"' tetraacetic acid (DOTA) (residualizing) (Chizzonite et al., 1991; Lombana et al., 2019). [^{125}I]-anti-Ly6E ADC was spiked into mouse plasma and incubated at 37^{o}C for 4 days to form A1M adduct in-vitro and [^{125}I]-anti-Ly6E mAb was treated similarly as control. All

DMD Fast Forward. Published on October 5, 2020 as DOI: 10.1124/dmd.120.000145
This article has not been copyedited and formatted. The final version may differ from this version.

radiolabeled materials were analyzed on an Agilent (Foster City, CA) high-performance liquid chromatography (HPLC) system 1100 series with a Phenomenex (Torrance, CA) Yarra S-3000 size-exclusion column – 3µM particle size, 7.8 x 3000 mm (SEC-HPLC), at isocratic flow rate of 0.5 mL/min of phosphate buffer saline (PBS) at pH 7.4 for 30 minutes. Radioactivity from the SEC-HPLC was detected by an in-line Raytest gamma detector (Elysia s.a., Angleur, Belgium). SEC-HPLC chromatogram profiles were compared to confirm the formation of A1M adduct.

In Vivo Studies

All in vivo PK studies in rodents were approved by the Institutional Animal Care and Use Committee at Genentech, Inc. and were conducted in compliance with the regulations of the Association for Assessment and Accreditation of Laboratory Animal Care.

PK studies of anti-Ly6E mAb and anti-Ly6E ADC in mice:

To evaluate the PK of anti-Ly6E mAb and anti-Ly6E ADC in mice, sixty female naive CB17 severe combined immunodeficient (SCID) mice (6-8 weeks old) were obtained from Charles River Laboratories, Inc. (Hollister, CA). Animals either received a single intravenous (IV) dose of 1 mg/kg of anti-Ly6E ADC or anti-Ly6E mAb via tail vein injection (N=30/group). Blood samples were collected from 3 mice in each dosing group at each of the following time points: 10 minutes, 1 and 6 hours, 1, 2, 3, 7, 10, 14, and 21 days. The sample collection was done via retro-orbital bleeds or cardiac puncture. Samples were processed to collect plasma and measure anti-Ly6E ADC or anti-Ly6E mAb antibody concentrations. Additionally, for the group receiving anti-Ly6E ADC,

DMD Fast Forward. Published on October 5, 2020 as DOI: 10.1124/dmd.120.000145
This article has not been copyedited and formatted. The final version may differ from this version.

samples were analyzed using the affinity capture assay to detect changes in the antibody molecular weight.

PK studies of anti-Ly6E mAb and anti-Ly6E ADC in rats:

To evaluate the PK of anti-Ly6E ADC and anti-Ly6E mAb in rats, nine female naïve Sprague-Dawley rats were obtained from Charles River Laboratories, Inc. (Hollister, CA) and split into two groups. Four rats received a single IV dose of anti-Ly6E mAb at 5 mg/kg of and five rats got a single IV dose of anti-Ly6E ADC at 2 mg/kg (lower ADC dose level used due to potential toxicity but not expected to interfere with PK in non-binding species) via the jugular vein cannula followed with a saline flush to clear the cannula. Blood samples were collected from each rat at each of the following time points: 10 minutes, 1 and 6 hours, 1, 3, 7, 10, 14, and 21 days. Rat blood samples were processed to collect plasma and measure total antibody level and changes in molecular weight using the affinity capture assay.

PK studies of anti-Ly6E mAb and anti-Ly6E ADC in cynomolgus monkeys:

These monkey studies were performed at Charles River Laboratories (Reno, NV) at different time. For the first study, 5 Cynomolgus monkeys were split into 2 groups, anti-Ly6E mAb was given as a single IV bolus administration at 0.3 (N=2) and 3 mg/kg (N=3), respectively. Blood samples were collected from the monkeys in each dosing group at each of the following time points: 15 minutes, 4 and 12 hours, 1, 3, 4, 7, 10, 14, 21, 28, 35, and 42 days. Monkey blood samples were processed to collect serum and measure anti-Ly6E mAb antibody level. For second monkey study, a total of ten monkeys were given multiple IV bolus administration of anti-Ly6E ADC at 2, 4, and 8

DMD Fast Forward. Published on October 5, 2020 as DOI: 10.1124/dmd.120.000145
This article has not been copyedited and formatted. The final version may differ from this version.

mg/kg every three weeks for four cycles (N=3 for 2 mg/kg, N=6 for 4 mg/kg, and N=1 for 8 mg/kg, respectively). Blood samples were collected at the following time-points after the first dose: pre-dose, 15 minutes, 1, 3, 7, 14, 21 post-doses. From the second to fourth cycles, blood samples were collected at the following time-points: 15 minutes, and 1, 3, 7, 14, 21 days post-dose. Blood samples were processed to collect plasma and used to measure anti-Ly6E ADC total antibody level and changes in molecular weight using the affinity capture assay. PK parameters were generated only using the first cycle total antibody concentration data for the anti-Ly6E ADC.

Tissue distribution study with radiolabeled ADC and mAb in tumor bearing SCID mice:

Eighty female naive C.B-17 SCID-beige mice (Charles River Lab, Hollister, CA) were inoculated with $5x10^6$ HCC1937X1 cells (a derivative from HCC1937 from ATCC) suspended in 0.1mL of Hanks' Balanced Salt Solution (HBSS) with matrigel in the thoracic mammary fat pad area. When the xenograft tumor reached the size of 200-300 mm^3, radiolabeled anti-Ly6E ADC or anti-Ly6E mAb (5 µCi of each radioprobe) was singly dosed IV at 2 different levels: radiolabeled tracer alone (at 0.05 mg/kg), or tracer + 0.4 mg/kg unlabeled materials (which sustain static tumor). For the tracer only groups, whole blood and tissues were collected at 1 and 6 hours, and 1, 3, and 7-days post-dosing (n=5 for each time point). Similarly, for the tracer + 0.4 mg/kg unlabeled material groups, whole blood and tissues were collected at 1 and 3-days post dosing (n=5 for each time point). Whole blood samples were processed for plasma and cell pellet. The collected tissues included tumor, liver, lungs, kidneys, heart, spleen, stomach, small intestine, large intestine, fat pad, and skin. After tissue collection, the tissues were rinsed with PBS pH

DMD Fast Forward. Published on October 5, 2020 as DOI: 10.1124/dmd.120.000145
This article has not been copyedited and formatted. The final version may differ from this version.

7.4, blotted dry, and weighed. All samples were analyzed for total radioactivity using a Perkin Elmer Wizard^2 gamma counter (Waltham, MA), and radioactivity data were calculated as percentage of injected dose (%ID) normalized by volume/weight (%ID/ml or %ID/g). Selected plasma samples were analyzed by the SEC-HPLC method as described in the radiolabeling section. SEC-HPLC chromatogram profiles were compared across time points.

Ex-vivo Formation of A1M-ADC Adduct and In Vitro Cell Binding Assay:

Anti-Ly6E ADC-A1M adduct was pre-formed by incubating [^{125}I]-radiolabeled-anti-Ly6E ADC (namely as **pre-formed A1M-ADC**) in mouse plasma at 37^{o}C for 4 days. As control, [^{125}I]-anti-Ly6E mAb was also incubated under the same condition (name as **preincubated mAb**). A1M adduct formation was characterized using SEC-HPLC showing about 50% (calculated as "area under the curve") as A1M-ADC whereas no A1M adduct formed for mAb (**Figure S1**).

For cell binding assay, HCC1937X1 cells (high Ly6E expression) or DOV13 cells (low Ly6E expression) were plated on 6 wells cell culture plate (costar) at ~0.5 x 10^6/well in Dulbecco's Modified Eagle's medium (DMEM) growth media with penicillin-streptomycin at 37^{o}C with 5% CO_2 overnight allowing cells to attach to the plates. Then, the growth media was replaced with 1mL of DMEM without antibiotic for 1 hour before adding radiolabeled molecules including preformed A1M-ADC adduct, preincubated mAb, anti-Ly6E ADC (no pre-plasma incubation), anti-Ly6E mAb (no pre-plasma incubation) or a non-targeted anti-gD mAb at ~0.15ug/mL (equivalent to ~0.1 µCi per well) in 50uL of mouse plasma. The cells were then incubated at 37^{o}C with 5% CO_2 for

DMD Fast Forward. Published on October 5, 2020 as DOI: 10.1124/dmd.120.000145
This article has not been copyedited and formatted. The final version may differ from this version.

3 hours. At the end of the incubation, the growth media was removed and the cells were washed with ice cold PBS for three times. Then the trypsinized cells were collected and analyzed for radioactivity on the gamma counter. The radioactivity was then converted as a percentage of total radioactivity added to the cells per well.

Bioanalysis of plasma samples

Anti-Ly6E mAb and anti-Ly6E ADC total antibody assay:

To determine anti-Ly6E ADC total antibody concentrations (in rodents and cynomolgus monkeys), as well as the anti-Ly6E mAb (in mice and monkeys), a specific peptide-based LC-MS/MS quantitative assay was used. Samples were enriched from mouse plasma via affinity capture using streptavidin magnetic beads coupled with biotinylated anti-human IgG antibody, and then subjected to "on-bead" proteolysis with trypsin. A representative signature tryptic peptide selected from the complementarity determining region (CDR) of Ly6E was identified as the surrogate for quantification of the antibody. The lower limit of quantitation (LLOQ) was 1 µg/mL in the LC-MS/MS assay. Similarly, to determine anti-Ly6E mAb in rats, a bridging ELISA technique (capturing via sheep anti–human IgG followed by detection using a sheep anti human IgG conjugated to horseradish peroxides) was employed, and the LLOQ was 0.02 µg/mL.

Affinity-capture LC-MS assay:

An affinity capture LC-MS assay was used to detect changes in molecular weight of the antibody as described (Su et al., 2019). Briefly, the biotinylated Ly6E receptor extracellular domain immobilized on streptavidin-coated magnetic beads was used to specifically capture various antibody species. The captured ADC was then eluted from

DMD Fast Forward. Published on October 5, 2020 as DOI: 10.1124/dmd.120.000145
This article has not been copyedited and formatted. The final version may differ from this version.

the beads and injected onto a reversed phased LC coupled to a Q-TOF mass spectrometer operated in the positive ESI mode. This hybrid LC-MS method, which is not quantitative, compared the ratio of the total ion current from the anti-Ly6E ADC and anti-Ly6E ADC adduct.

Pharmacokinetic (PK) and statistical analysis:

Total antibody plasma concentration–time profiles for anti-Ly6E mAb and anti-Ly6E ADC, were used to estimate the following PK parameters in mouse, rat, and cynomolgus monkey, using non-compartmental analysis in Phoenix 1.4 (WinNonlin PK software version 6.4, Certara, USA):

$AUC_{INF}^{TAB}/Dose$: area under the total antibody concentration–time curve extrapolated to infinity normalized by dose

$C_{max}^{TAB}/Dose$: observed total antibody maximum serum concentration

CL^{TAB} : total antibody clearance

V_{ss}^{TAB} : total antibody volume of distribution at steady state

t_{half}^{TAB} : total antibody terminal half-life

A naïve pooled approach was used in the analysis of mouse studies to provide one estimate for each dose group. For the analysis of rat and monkey data, each animal was analyzed separately and results for each dose group were summarized as mean ± standard deviation (SD). Due to the nature and study design of the PK studies, no formal statistical analysis was performed to determine the significance of the difference in PK exposure of anti-Ly6E mAb and anti-Ly6E ADC as these studies were not powered for statistical analysis. Instead, only a post-hoc exploratory statistical analysis was done for

DMD Fast Forward. Published on October 5, 2020 as DOI: 10.1124/dmd.120.000145
This article has not been copyedited and formatted. The final version may differ from this version.

PK parameters from rats and monkeys to compare the C_{max}/dose and AUC_{INF}/dose between the anti-Ly6E ADC and anti-Ly6E mAb but the data was not reported in the manuscript due to the limited study power.

Results

Mouse PK:

The PK of anti-Ly6E mAb and anti-Ly6E ADC was examined in CB17 SCID mice (non-binding species). The total antibody plasma concentration-time profiles of anti-Ly6E mAb and anti-Ly6E ADC following a single IV bolus dose in CB17 SCID mice at 1 mg/kg are shown in **Figure 2** and the corresponding PK parameters are summarized in **Table 1**. Measured values of the dosing solutions were within acceptable range (±20%), therefore nominal doses were used for the PK analysis. Both anti-Ly6E mAb and anti-Ly6E ADC exhibited bi-exponential disposition with comparable values of dose normalized C_{max} (24.0 and 26.1 [µg/mL]/[mg/kg] for anti-Ly6E mAb and anti-Ly6E ADC, respectively). The estimated values for the dose normalized AUC_{INF} appeared to be higher for the anti-Ly6E ADC versus the mAb with values of 300 versus 244 [day• µg/mL]/[mg /kg], respectively; however, a high fraction (>30%) of the total area was extrapolated to compute these values so they must be interpreted with caution. Accordingly, the clearance values for the anti-Ly6E ADC versus the mAb were estimated as 3.33 and 4.12 [mL/day/kg], consistent with the apparent higher exposure of the ADC versus the mAb. Differences in the calculated V_{ss} values (85.5 [mL/kg] for anti-Ly6E

DMD Fast Forward. Published on October 5, 2020 as DOI: 10.1124/dmd.120.000145
This article has not been copyedited and formatted. The final version may differ from this version.

mAb versus 59.7 [mL/kg] for the anti-Ly6E ADC) suggest that anti-Ly6E mAb has a higher volume of distribution than anti-Ly6E ADC.

Rat PK:

The PK of anti-Ly6E mAb and anti-Ly6E ADC were also examined in a second non-binding species Sprague Dawley rats. Total antibody plasma concentration-time profiles following the administration of a single IV bolus of 2 mg/kg of anti-Ly6E mAb and 5 mg/kg of anti-Ly6E ADC (dose normalized to 5 mg/kg) are shown in **Figure 3** and the corresponding PK parameters are summarized in **Table 1**. Both molecules show bi-exponential PK similar to that in mice. Values of the dose normalized C_{max} (25.2 versus 28.2 [µg/mL]/[mg/kg] for the mAb and the ADC, respectively) and dose-normalized AUC_{INF} (161 versus 194 day• [µg/mL]/[mg/kg] for the mAb and the ADC, respectively) are comparable for both test articles. The estimated clearance values were 6.97 [mL/day/kg] for anti-Ly6E mAb and 5.87 [mL/day/kg] for anti-Ly6E ADC. While this study was not powered for statistical analysis, a post-hoc exploratory statistical analysis was done on rat PK parameters comparing the C_{max}/dose and AUC_{INF}/dose between the anti-Ly6E ADC and anti-Ly6E mAb. The results were not statistically significant ($p>0.05$) in rats (data not shown).

Monkey PK:

After a single IV administration of 0.3 or 3 mg/kg of anti-Ly6E mAb, dose normalized AUC_{INF} were 222 and 256 ± 14.0 day • [µg/mL]/[mg/kg], respectively, suggesting roughly dose-proportional PK behavior within the dose range tested. The mean clearance values of anti-Ly6E mAb were 4.51 and 3.92 [mL/day/kg], respectively. The PK

DMD Fast Forward. Published on October 5, 2020 as DOI: 10.1124/dmd.120.000145
This article has not been copyedited and formatted. The final version may differ from this version.

parameters derived for anti-Ly6E mAb were as expected for a human IgG1 mAb in cynomolgus monkeys and consistent with other typical IgG1 mAbs developed by Genentech, Inc. (Deng et al., 2011).

Anti-Ly6E ADC is expected to bind to cynomolgus monkey Ly6E since conjugation of payload at K149C site is not anticipated to alter antibody-target interaction (Leipold et al., 2018). Anti-Ly6E ADC shows a comparable dose normalized C_{max} (26.0, 26.0, and 23.9 [ug/mL]/[mg/kg]) and dose normalized AUC_{INF} (177, 205, and 157 day• [µg/mL]/ [mg /kg]) across the dose range tested, suggesting a linear PK behavior across this dose range (at 2, 4, and 8 mg/kg). The respective mean clearance estimates were 5.78, 6.82, and 6.38 [mL/day/kg] at 2, 4, and 8 mg/kg dose, respectively. All dosing solutions were within acceptable range (± 20%). The dose normalized total antibody PK profiles following the administration of anti-Ly6E ADC (first cycle) and anti-Ly6E mAb to cynomolgus monkeys are shown in **Figure 4**. Individual dose group's concentration-time profiles for monkey are shown in **Supplement Figure 2**. The corresponding non-compartmental PK parameters are summarized in **Table 2**. Post-hoc exploratory statistical analysis was also done for monkey PK parameters comparing the C_{max}/dose and AUC_{INF}/dose between the anti-Ly6E ADC and anti-Ly6E mAb. The results were modestly statistically significant ($0.01<p<0.05$) in monkeys (data not shown).

Different rate and extent of A1M adduct formation across species in-vivo:

ADCs carrying a CBI-dimer payload (e.g. anti-Ly6E ADC) is known to undergo major bio-transformations via payload-protein adduct formation, resulting in attenuation of ADC activity (Su et al., 2019). We have analyzed plasma samples from mice, rats, and monkeys following anti-Ly6E ADC administration to detect formation of ~~the~~ A1M

DMD Fast Forward. Published on October 5, 2020 as DOI: 10.1124/dmd.120.000145
This article has not been copyedited and formatted. The final version may differ from this version.

adduct by using a MS-affinity capture assay and explore if the appearance of the A1M adduct is associated with changes on PK and/or biodistribution of the molecule. In CB17 SCID mouse, adduct (+24.2 kDa) was detected as early as 1 hour after dosing and became dominant by 24 hours (**Figure 5A**). Similarly, affinity capture assay also showed the formation of A1M adduct (+23.3 kDa) at 6 hours post dosing and became the dominant species on day 7 post dosing. One of these rats received anti-Ly6E ADC dosing showed much higher exposure than the other rats; co-incidentally, this rat also showed higher extent of A1M adduct. In contrast, in cynomolgus monkeys, A1M adduct (+25.9 kDa) was detected at 24 hours post dosing at 2 mg/kg and 72 hours after dosing at 4 mg/kg. It took around 7 days for A1M adduct to become the dominant species after anti-Ly6E ADC administration (**Figure 5B**). Taken together, these data suggest that A1M adduct formation occurs most rapidly with higher extent in mice followed by rats as compared to that in monkeys. Thus, the rate and extent of A1M adduct formation appeared to inversely correlate with ADC Tab clearance.

Anti-Ly6E ADC trends to have reduced tissue distribution with striking reduction to tumors in mice:

Following dosing of radiolabeled-ADC in tumor bearing mice, plasma radioactivity levels were higher than that in mice dosed with radiolabeled-mAb, consistent with PK study in mice. SEC-HPLC analysis revealed that the retention time of main peak shifted to the left for ADC samples, but not for mAb samples (**Figure 6**), indicating the formation of A1M adduct with ADC as seen in previous analysis.

DMD Fast Forward. Published on October 5, 2020 as DOI: 10.1124/dmd.120.000145
This article has not been copyedited and formatted. The final version may differ from this version.

Measurement of tissue radioactivity demonstrated that anti-Ly6E ADC trended to have overall lower tissue radioactivity levels than that for anti-Ly6E mAb throughout the study course though the difference was not significant (**Figure 7**). At 3 days after dosing, liver, kidneys, and spleen (non-targeted tissues) have a total ^{111}In radioactivity level of 21.5 %ID/g for anti-Ly6E ADC vs 30.7 %ID/g for anti-Ly6E mAb. However, anti-Ly6E ADC showed a striking reduction to tumors in comparison to mAb. As shown in Figure 6A, tumor radioactivity levels in mice dosed with radiolabeled-ADC were significantly lower than that seen in mice dosed with radiolabeled-mAb over the study course of 7 days. On day 1 post-dosing, the ^{111}In radioactivity in tumor for animals dosed with anti-Ly6E ADC was 10.0 ± 1.95 %ID/g vs. 17.3 ± 1.10 %/ID/g for animals dosed with radiolabeled-anti-Ly6E mAb. On day 3 post-dosing, the tumor radioactivity from the anti-Ly6E ADC group was around 9.90 (± 2.12) %ID/g as compared to 20.4 (± 3.78) %ID/g in tumor from animals dosed with anti-Ly6E mAb group (**Figure 7**). The trend continued to the end of the study course.

To further understand the extent of molecule internalization and catabolism, we have analyzed the difference between ^{111}In and ^{125}I radioprobes. While both probes can be used to assess the tissue distribution, only ^{125}I can be released back to extracellular space after the intracellular degradation of antibody while ^{111}In residualized inside cells as the DOTA can't cross the cell membrane. Side by side comparison of the radioactivity from these two probes in different tissues not only enabled us to monitor the tissues distribution, but also helped evaluate the site where internalization and catabolism occurred. In our result, there was little difference between ^{125}I and ^{111}In radioactivity in tumor tissues dosed with anti-Ly6E ADC (Δ of 1.36% and 2.41% ID/g for 1 day and 3

DMD Fast Forward. Published on October 5, 2020 as DOI: 10.1124/dmd.120.000145
This article has not been copyedited and formatted. The final version may differ from this version.

days post-dosing, respectively), whereas there was a much greater difference between the two radioprobes in tumor dosed with anti-Ly6E mAb ((Δ of 6.34% and 9.26% ID/g for 1 day and 3 days post-dosing, respectively). This result indicated that little anti-Ly6E ADC was internalized into the tumors as compared to anti-Ly6E mAb (**Figure 7**). Consistently, co-dosing with excess amount of unlabeled ADC materials did not appear to impact tumor distribution, indicating that there was no displacement of specific target binding, therefore formation of A1M adduct alters the specific tumor distribution.

Anti-Ly6E ADC A1M-adduct showed reduced target binding in tumor cells in vitro:

To further understand whether A1M adduct formation would interfere with cell binding, A1M adduct of ADC was pre-formed as described in "Methods" and then incubated in cell line that either expressing high (HCC1937X1) or low (DOV13) level of Ly6E antigen. As shown in **Figure 8**, the total radioactivity in cells treated with control anti-Ly6E ADC (no preincubation with plasma, thus no A1M adduct formation) was similar to that of cells treated with anti-Ly6E mAb (also no preincubation with plasma and no A1M adduct formation) (0.760 ± 0.0281% for anti-Ly6E mAb vs. 0.708 ± 0.0744% for anti-Ly6E ADC in HCC1937X1 and 0.313 ± 0.0514% for anti-Ly6E mAb vs. 0.334 ± 0.0469% for anti-Ly6E ADC in DOV13) after 3 hours of incubation. However, cellular radioactivity following treatment with preformed A1M-ADC group (preincubated with plasma to form A1M adduct) was significantly lower ($p<0.01$) than preincubated mAb group (anti-Ly6E mAb that was pre-incubated in plasma) in both cell line after 3 hours of incubation (0.602 ± 0.0876% for preincubated mAb vs. 0.437 ± 0.0201% for preformed A1M-ADC in HCC1937X1 and 0.350 ± 0.0718% for

preincubated mAb vs. 0.197 ± 0.0473% for preformed A1M-ADC in DOV13) (**Figure 8**). As expected, the cellular radioactivity in HCC1937X1 (higher Ly6E expression) cell line was higher than DOV13 (lower Ly6E expression) for anti-Ly6 E mAb under both conditions (i.e. with or without preincubation with plasma). The non-targeted antibody, anti-gD, had the lowest radioactivity binding and uptake in both cell lines.

Discussion

The PK of ADCs has been described in multiple publications previously (Hamblett, 2004; Boswell, 2011; Lin, 2013; Kamath, 2015; Leipold, 2018). In general, the systemic clearance of ADCs trends to be faster than that of the unconjugated mAbs attributed to the "impact of conjugation" (Boswell, 2011). Higher hydrophobicity, emerging pockets of increased electrostatic or altered FcRn binding upon conjugation of the payload all could potentially cause higher CL of ADC (Boswell, 2011; Kamath, 2015). However, the impact of conjugation on ADC clearance is expected to differ in magnitude with different types of payload, linker, and conjugation technologies. In addition, ADC may undergo biotransformation such as interacting with plasma protein, which may further complicate the impact on ADC clearance.

Anti-Ly6E-*seco*-CBI dimer ADC was previously reported to form an adduct with A1M in animal plasma in circulation once the phosphate group was removed by phosphatase and the payload rearranged molecularly to become biologically active (Su, 2019). The binding of A1M to one of CBI-dimer appeared to attenuate ADC's activity in an *in-vitro*

DMD Fast Forward. Published on October 5, 2020 as DOI: 10.1124/dmd.120.000145
This article has not been copyedited and formatted. The final version may differ from this version.

assay, likely due to reduced DNA alkylation, as such attenuating its activity (Purnell, 2006). However, the impact of A1M adduct formation on ADC PK and tissue distribution is not fully understood, which may also affect ADC activity and its developability.

In the current study, we have compared the PK of anti-Ly6E ADC Tab (forming A1M adduct) with anti-Ly6E mAb (no A1M adduct formation) in mice, rats (both non-binding species), and cynomolgus monkeys (binding species). The clearance of ADC Tab was slower than that of mAb in mice (3.33vs. 4.12 [mL/day/kg] for ADC and mAb, respectively) and rats (5.87 ± 1.88 vs. 6.97 ± 2.60 [mL/day/kg] for ADC and mAb, respectively) (**Table 1**). Unlike mice and rats, the clearance for ADC in cynomolgus monkey was faster than that of mAb at both 2 and 4 mg/kg (5.78± 1.10 and 6.82± 1.13 [mL/day/kg], respectively). In contrast, the clearance of mAb at 3mg/kg in monkeys was 3.92 ± 0.221 [mL/day/kg], which was slower than that of either 2 or 4 mg/kg of ADC in monkeys (**Table 2**).

We hypothesized that the rate and extent of A1M adduct formation may differ between rodents and monkeys, leading to the different ADC clearance. As such, we compared the relative adduct formation rate and extent in plasma from mice, rats and monkeys using the affinity capture assay. The results revealed that the rate of A1M adduct formation inversely correlated with the clearance of anti-Ly6E ADC. The A1M adduct formation was most rapid in mouse plasma. It became dominant (greater than 80% of ion intensity observed by affinity-LC/MS with +24kDa) within 24 hours following dosing. In contrast

DMD Fast Forward. Published on October 5, 2020 as DOI: 10.1124/dmd.120.000145
This article has not been copyedited and formatted. The final version may differ from this version.

to mice, the formation of A1M adduct in monkeys was much slower and took 7 days to become dominant (greater than 80% of ion intensity with +26kDa). This is consistent with the results reported by Su et al. for anti-CD22-seco-CBI dimer ADC (with same linker-payload that also forms A1M adduct) (Su, 2019). These data indicated that the A1M adduct formation could reduce the clearance of anti-Ly6E ADC, particularly in rodents that have higher level and rapid formation of A1M adduct in plasma following IV dosing. Presently, it is unknown why the rate and extent of A1M adduct formation with ADC are different between rodents and monkeys. A1M is known to be highly heterogeneous with different molecule size and abundance between rodent and monkey (Akerström, 1985), which may contribute to the discrepancy in A1M-ADC adduct formation between rodent and monkey. This data also brings up a challenge in translating the PK for this ADC across animal species.

In general, the complex formation of biologics is expected to enhance its clearance due to an increase in the molecular size that would trigger the uptake and degradation of high molecular complexes by the reticuloendothelial system. However, here we have observed a paradoxical effect of complex formation on clearance. Since tissue disposition is known to play a key role in driving systemic clearance of antibody, we have further assessed whether the A1M adduct formation would alter the normal tissue (non-target mediated) and tumor (target specific mediated) distribution of anti-Ly6E-ADC in a tumor-bearing mouse model by comparing with the tissue disposition profiles of unconjugated mAb. Following administration of [^{125}I]- and [^{111}In]-anti-Ly6E ADC or [^{125}I]- and [^{111}In]-anti-Ly6E mAb into mice bearing high Ly6E expression tumor

DMD Fast Forward. Published on October 5, 2020 as DOI: 10.1124/dmd.120.000145
This article has not been copyedited and formatted. The final version may differ from this version.

xenograft model, the plasma radioactivity levels in mice dosed with anti-Ly6E ADC were higher than that from mice dosed with anti-Ly6E mAb, consistent with PK results in mice. SEC-HPLC analysis confirmed that A1M adduct was only seen in plasma samples dosed with anti-Ly6E ADC but not in samples dosed with anti-Ly6E mAb. Analysis of tissue radioactivity demonstrated that overall the tissue radioactivity levels in mice dosed with anti-Ly6E ADC trended to be lower than that detected in mice dosed with anti-Ly6E mAb (**Figure 7B**). Though no individual tissue showed statistical difference, the overall totality of the differences from all tissues may explain, at least in part, the lower systemic clearance of this ADC, implying that the A1M adduct formation of ADC may impact non-target mediated tissue uptake. It is currently unknown how the A1M adduct formation alters the non-specific tissue uptake. One possibility may be due to the adduct formation changing the physical-chemical properties of ADC such as charge or hydrophobicity, which needs to be further investigated.

To understand whether A1M adduct formation would impact specific target mediated tissue distribution, we have further determined the tumor distribution in a tumor bearing mice model. To our surprise, anti-Ly6E ADC showed a strikingly reduced tumor tissue distribution as compared to unconjugated mAb. As shown in Fig 6, the ^{111}In radioactivity amount detected in tumors from mice dosed with anti-Ly6E ADC after one day was about 2 folds lower than that seen in the tumors from mice dosed with anti-Ly6E mAb. This profile is in accordance with the formation of A1M adduct in plasma from mice dosed with anti-Ly6E ADC. In addition, both residualizing ^{111}In and non-residualizing ^{125}I probes equally showed a low uptake of radioactivity into tumor tissues. The intact

DMD Fast Forward. Published on October 5, 2020 as DOI: 10.1124/dmd.120.000145
This article has not been copyedited and formatted. The final version may differ from this version.

molecules are represented by the non-residualized probe, iodine-125, since this probe would be eliminated from circulation once molecules get internalized and catabolized by the lysosomes, while the residualizing probe, DOTA-indium-111, would represent both the intact molecules and any catabolized molecule. Also, co-dosing with an excess amount of unlabeled ADC did not appear to alter tumor radioactivity. Together, these data indicate that the A1M adduct formation of ADC resulted in little specific distribution or internalization into tumor tissues even though systemic exposure is higher.

We hypothesized that the A1M adduct formation with ADC may interfere with the target antigen binding. To test this hypothesis, the uptake of preformed [^{125}I]-A1M-ADC adduct and [^{125}I]-anti-Ly6E mAb was assessed in cell line that express either high Ly6E (HCC1937X1) or low Ly6E expression (DOV13). While the uptake of non-incubated [^{125}I]-anti-Ly6E ADC (i.e. no A1M adduct formation) and [^{125}I]-anti-Ly6E mAb was similar, the preformed A1M-ADC showed a much lower uptake than that of preincubated mAb (also preincubated in plasma). The reduction of A1M-ADC uptake was more pronounced in high Ly6E expressing HCC1937X1 cell line than the low Ly6E expression DOV13 cell line, which further support that the A1M adduct formation could interfered with the target binding of anti-Ly6E ADC. This is consistent with the in vivo data that showed little internalization as both residualizing ^{111}In and non-residualizing ^{125}I probes had similar lower distribution to tumors. These data demonstrate that the A1M adduct formation of anti-Ly6E ADC could reduce the tumor distribution likely through interfering with antigen target binding/recognition. One possibility is that A1M adduct formation with anti-Ly6E ADC may change the steric hindrance of the binding site,

DMD Fast Forward. Published on October 5, 2020 as DOI: 10.1124/dmd.120.000145
This article has not been copyedited and formatted. The final version may differ from this version.

leading to masking the binding site on the CDR region, as such blocking the antigen binding. Further study will be needed to elucidate the exact molecular mechanism on how A1M adduct formation interferes with antigen binding. Previous study (Su, 2019) showed that an anti-CD22 mAb conjugated with the same CBI-dimer payload also formed an adduct with A1M. Therefore, the A1M adduct formation appears to be independent of antibody target rather than a linker-drug specific issue. Limited in vitro data indicated that the *seco*-CBI-Dimer ADCs are likely to form adduct with A1M if administered into human (Su, 2019). Thus, a similar impact on ADC PK and tumor distribution is expected. Unfortunately, this ADC was not moved forward to humans.

In conclusion, we have investigated the impact of A1M adduct formation on PK and tissue distribution of anti-Ly6E -*seco*-dimer ADC in rodents and monkeys. Our data demonstrated that A1M adduct formation of anti-Ly6E ADC could reduce the total antibody clearance dependent on A1M adduct formation rate and extent. Though increasing the systemic exposure, A1M-adduct formation showed a striking reduction in tumor distribution, probably due to interfering with target antigen binding. These findings highlight the importance of selecting/optimizing the linker-drug structure for ADC molecules given its complexity and emphasize the value of conducting mechanistic understanding of ADC biotransformation in early stages of ADC development.

Acknowledgements

The authors would like to thank the In Vivo Study Group at Genentech for conducting all in vivo studies. We also want to thank Pete Dragovich, Dian Su, and Tom Pillow for providing very insightful discussion and constructive feedback on the manuscript. Anshin Biosolution provided some help with manuscript editing.

Authorship contributions:

Participated in study design: Yip, Figueroa, Kamath, and Shen

Conducted experiments and sample analysis: Yip and Ng

Performed data analysis: Yip, Figueroa, Latifi, Maish, Leipold, and Ng

Wrote or contributed to writing of the manuscript: Yip, and Shen

References:

Abdollahpour-Alitappeh M, Lotfinia M, Gharibi T, Mardaneh J, Farhadihosseinabadi B, Larki P, Faghfourian B, Sepehr KS, Abbaszadeh-Goudarzi K, Abbaszadeh-Goudarzi G, Johari B, Zali MR, and Bagheri N (2019) Antibody-drug conjugates (ADCs) for cancer therapy: Strategies, challenges, and successes. *J Cell Physiol* **234:**5628-5642.

AlHossiny M, Luo L, Frazier WR, Steiner N, Gusev Y, Kallakury B, Glasgow E, Creswell K, Madhavan S, Kumar R, and Upadhyay G (2016) Ly6E/K Signaling to TGFβ Promotes Breast Cancer Progression, Immune Escape, and Drug Resistance. *Cancer Res* **76:**3376-3386.

Akerström B **(**1985) Immunological Analysis of Alpha 1-microglobulin in Different Mammalian and Chicken Serum. Alpha 1-Microglobulin Is 5-8 Kilodaltons Larger in Primates. *J Biol Chem* 260(8):4839-44.

Asundi J, Crocker L, Tremayne J, Chang P, Sakanaka C, Tanguay J, Spencer S, Chalasani S, Luis E, Gascoigne K, Desai R, Raja R, Friedman BA, Haverty PM, Polakis P, and Firestein R (2015) An Antibody-Drug Conjugate Directed against Lymphocyte Antigen 6 Complex, Locus E (LY6E) Provides Robust Tumor Killing in a Wide Range of Solid Tumor Malignancies. *Clin Cancer Res* **21:**3252-3262.

Birrer MJ, Moore KN, Betella I, and Bates RC (2019) Antibody-Drug Conjugate-Based Therapeutics: State of the Science. *J Natl Cancer Inst*.

Boswell CA, Mundo EE, Zhang C, Bumbaca D, Valle NR, Kozak KR, Fourie A, Chuh J, Koppada N, Saad O, Gill H, Shen BQ, Rubinfeld B, Tibbitts J, Kaur S, Theil FP, Fielder PJ, Khawli LA, and Lin K (2011) Impact of drug conjugation on pharmacokinetics and tissue distribution of anti-STEAP1 antibody-drug conjugates in rats. *Bioconjug Chem* **22:**1994-2004.

Chizzonite R, Truitt T, Podlaski FJ, Wolitzky AG, Quinn PM, Nunes P, Stern AS, and Gately MK (1991) IL-12: monoclonal antibodies specific for the 40-kDa subunit block receptor binding and biologic activity on activated human lymphoblasts. *J Immunol* **147:**1548-1556.

Deng R, Iyer S, Theil FP, Mortensen DL, Fielder PJ, and Prabhu S (2011) Projecting human pharmacokinetics of therapeutic antibodies from nonclinical data: what have we learned? *MAbs* **3:**61-66.

Diamantis N and Banerji U (2016) Antibody-drug conjugates--an emerging class of cancer treatment. *Br J Cancer* **114:**362-367.

Frigerio M and Kyle AF (2017) The Chemical Design and Synthesis of Linkers Used in Antibody Drug Conjugates. *Curr Top Med Chem* **17:**3393-3424.

Garon EB, Hellmann MD, Rizvi NA, Carcereny E, Leighl NB, Ahn MJ, Eder JP, Balmanoukian AS, Aggarwal C, Horn L, Patnaik A, Gubens M, Ramalingam SS, Felip E, Goldman JW, Scalzo C, Jensen E, Kush DA, and Hui R (2019) Five-Year Overall Survival for Patients With Advanced NonSmall-Cell Lung Cancer Treated With Pembrolizumab: Results From the Phase I KEYNOTE-001 Study. *J Clin Oncol* **37:**2518-2527.

Hamblett KJ, Senter PD, Chace DF, Sun MM, Lenox J, Cerveny CG, Kissler KM, Bernhardt SX, Kopcha AK, Zabinski RF, Meyer DL, and Francisco JA (2004) Effects of drug loading on the antitumor activity of a monoclonal antibody drug conjugate. *Clin Cancer Res* **10:**7063-7070.

Inthagard J, Edwards J, and Roseweir AK (2019) Immunotherapy: enhancing the efficacy of this promising therapeutic in multiple cancers. *Clin Sci (Lond)* **133:**181-193.

Jin HT, Ahmed R, and Okazaki T (2011) Role of PD-1 in regulating T-cell immunity. *Curr Top Microbiol Immunol* **350:**17-37.

Junutula JR, Bhakta S, Raab H, Ervin KE, Eigenbrot C, Vandlen R, Scheller RH, and Lowman HB (2008a) Rapid identification of reactive cysteine residues for site-specific labeling of antibody-Fabs. *J Immunol Methods* **332:**41-52.

Junutula JR, Raab H, Clark S, Bhakta S, Leipold DD, Weir S, Chen Y, Simpson M, Tsai SP, Dennis MS, Lu Y, Meng YG, Ng C, Yang J, Lee CC, Duenas E, Gorrell J,

Katta V, Kim A, McDorman K, Flagella K, Venook R, Ross S, Spencer SD, Lee Wong W, Lowman HB, Vandlen R, Sliwkowski MX, Scheller RH, Polakis P, and Mallet W (2008b) Site-specific conjugation of a cytotoxic drug to an antibody improves the therapeutic index. *Nat Biotechnol* **26:**925-932.

Kamath AV and Iyer S (2015) Preclinical Pharmacokinetic Considerations for the Development of Antibody Drug Conjugates. *Pharm Res* **32:**3470-3479.

Leipold DD, Figueroa I, Masih S, Latifi B, Yip V, Shen BQ, Dere RC, Carrasco-Triguero M, Lee MV, Saad OM, Liu L, He J, Su D, Xu K, Vuillemenot BR, Laing ST, Schutten M, Kozak KR, Zheng B, Polson AG, and Kamath AV (2018) Preclinical pharmacokinetics and pharmacodynamics of DCLL9718A: An antibody-drug conjugate for the treatment of acute myeloid leukemia. *MAbs* **10:**1312-1321.

Lin K, Tibbitts J., Shen BQ. (2013) Pharmacokinetics and ADME Characterizations of Antibody–Drug Conjugates. In: Ducry L. (eds) Antibody-Drug Conjugates. Methods in Molecular Biology (Methods and Protocols), vol 1045. Humana Press, Totowa, NJ.

Lombana TN, Rajan S, Zorn JA, Mandikian D, Chen EC, Estevez A, Yip V, Bravo DD, Phung W, Farahi F, Viajar S, Lee S, Gill A, Sandoval W, Wang J, Ciferri C, Boswell CA, Matsumoto ML, and Spiess C (2019) Production, characterization, and in vivo half-life extension of polymeric IgA molecules in mice. *MAbs* **11:**1122-1138.

Lu D, Sahasranaman S, Zhang Y, and Girish S (2013) Strategies to address drug interaction potential for antibody-drug conjugates in clinical development. *Bioanalysis* **5:**1115-1130.

Miliotou AN and Papadopoulou LC (2018) CAR T-cell Therapy: A New Era in Cancer Immunotherapy. *Curr Pharm Biotechnol* **19:**5-18.

Ohri R, Bhakta S, Fourie-O'Donohue A, Dela Cruz-Chuh J, Tsai SP, Cook R, Wei B, Ng C, Wong AW, Bos AB, Farahi F, Bhakta J, Pillow TH, Raab H, Vandlen R, Polakis P, Liu Y, Erickson H, Junutula JR, and Kozak KR (2018) High-Throughput Cysteine Scanning To Identify Stable Antibody Conjugation Sites for Maleimide- and Disulfide-Based Linkers. *Bioconjug Chem* **29:**473-485.

Palleria C, Di Paolo A, Giofre C, Caglioti C, Leuzzi G, Siniscalchi A, De Sarro G, Gallelli L (2012) Pharmacokinetics drug-drug interactaion and their implication in clinical management. *J Res Med Sci.* **18(7):**601-10.

Parrish JP, Kastrinsky DB, Stauffer F, Hedrick MP, Hwang I, and Boger DL (2003) Establishment of substituent effects in the DNA binding subunit of CBI analogues of the duocarmycins and CC-1065. *Bioorg Med Chem* **11:**3815-3838.

Seimetz D, Heller K, and Richter J (2019) Approval of First CAR-Ts: Have we Solved all Hurdles for ATMPs? *Cell Med* **11:**2155179018822781.

Sousa M, Pozniak A, and Boffito M (2008) Pharmacokinetics and pharmacodynamics of drug interactions involving rifampicin, rifabutin and antimalarial durgs. *J Antimicrob Chemother.* **62(5)**:872-8

Su D, Chen J, Cosino E, Dela Cruz-Chuh J, Davis H, Del Rosario G, Figueroa I, Goon L, He J, Kamath AV, Kaur S, Kozak KR, Lau J, Lee D, Lee MV, Leipold D, Liu L, Liu P, Lu GL, Nelson C, Ng C, Pillow TH, Polakis P, Polson AG, Rowntree RK, Saad O, Safina B, Stagg NJ, Tercel M, Vandlen R, Vollmar BS, Wai J, Wang T, Wei B, Xu K, Xue J, Xu Z, Yan G, Yao H, Yu SF, Zhang D, Zhong F, and

Dragovich PS (2019) Antibody-Drug Conjugates Derived from Cytotoxic *seco*-CBI-Dimer Payloads Are Highly Efficacious in Xenograft Models and Form Protein Adducts In Vivo. *Bioconjug Chem* **30:**1356-1370.

Su D, Kozak KR, Sadowsky J, Yu SF, Fourie-O'Donohue A, Nelson C, Vandlen R, Ohri R, Liu L, Ng C, He J, Davis H, Lau J, Del Rosario G, Cosino E, Cruz-Chuh JD, Ma Y, Zhang D, Darwish M, Cai W, Chen C, Zhou H, Lu J, Liu Y, Kaur S, Xu K, and Pillow TH (2018) Modulating Antibody-Drug Conjugate Payload Metabolism by Conjugation Site and Linker Modification. *Bioconjug Chem* **29:**1155-1167.

Footnotes

All works in this manuscript is funded and supported by Genentech (a Roche's company).

DMD Fast Forward. Published on October 5, 2020 as DOI: 10.1124/dmd.120.000145
This article has not been copyedited and formatted. The final version may differ from this version.

Figure legends

Figure 1. Anti-Ly6E ADC (DAR of 2) with the structure of the linker-payload (*seco*-cyclopropabenzindol-4-one (*seco*-CBI) dimer). After the payload lose its phosphate group by the phosphatase in circulation, it rearranged molecularly into the biologically active form of CBI-dimer where the Alpha-1-microglobulin (A1M) or other plasma proteins alkylate to the conjugated CBI-dimer through its electrophilic moieties forming the adduct (Su et al., 2019).

Figure 2. Mean (± SD) antibody concentration-time profiles of anti-Ly6E ADC and anti-Ly6E mAb following a single IV administration in female CB17 SCID mice (N=3).

SD, standard deviation; Ly6E, Lymphocyte antigen 6 complex, locus E; IV, intravenous

Figure 3. Mean (± SD) antibody concentration-time profiles (dose normalized) of anti-Ly6E ADC and anti-Ly6E mAb following a single IV administration (2mg/kg for ADC and 5mg/kg for mAb) in Sprague-Dawley rats (N=4 for ADC and N=5 for mAb).

SD, standard deviation; Ly6E, Lymphocyte antigen 6 complex, locus E; mAb, monoclonal antibody; IV, intravenous

Figure 4. Mean (± SD) antibody concentration-time profiles (dose normalized) of anti-Ly6E ADC from first cycle following multiple IV doses (Q3w) and anti- Ly6E mAb

following a singly IV dosing in cynomolgus monkeys. Anti-Ly6E ADC was dosed at 2, 4, and 8mg/kg and anti-Ly6E mAb was dosed at 0.3 and 3 mg/kg (For ADC, N=3, 6, & 1 for 2, 4, and 8 mg/kg respectively; For mAb, N=2 and 3 for 0.3 and 3 mg/kg).

SD, standard deviation; Ly6E, Lymphocyte antigen 6 complex, locus E; Q3w, every three weeks; ADC, antibody-drug conjugate; IV, intravenous

Figure 5. Analysis of anti-Ly6E ADC-A1M adduct formation in mouse and monkey plasma using Affinity-capture LC-MS analysis of representative plasma sample. **(A)** DAR distribution and A1M adduct formation of anti-Ly6E ADC in mouse plasma. A1M adduct (+24.2 kDa) was detected in mouse plasma one hour after dosing and became dominant by 24 hours; no significant deconjugation (maleimide exchange) was observed. **(B)** Analysis of DAR distribution and A1M adduct formation of anti-Ly6E ADC in monkey plasma. A1M adduct (+ ~26 kDa) was detected in monkey plasma at 24, 72, and 168 hours after dosing at both dosing levels (2 and 4 mg/kg).

Ly6E, Lymphocyte antigen 6 complex, locus E; ADC, antibody-drug conjugate; A1M, alpha-1-microglobulin; LC-MS, liquid chromatography – mass spectrometry; DAR, drug-to-antibody ratio

Figure 6. Analysis of A1M adduct formation following dosing radiolabeled anti-Ly6E ADC or anti-Ly6E mAb using SEC-HPLC with in-line radio-detector. **(A)** Baseline profiles of [^{125}I] radiolabeled anti-Ly6E ADC (blue) and anti-Ly6E mAb (red) dosing materials showing the same retention time. **(B)** At 1-hour post dose, retention time of the

DMD Fast Forward. Published on October 5, 2020 as DOI: 10.1124/dmd.120.000145
This article has not been copyedited and formatted. The final version may differ from this version.

main peak shifted to the left for anti-Ly6E ADC plasma while remained the same for anti-Ly6E mAb, indicating the formation of A1M adduct in anti-Ly6E ADC plasma (only representative plasma samples analyzed).

A1M, alpha-1-microglobulin; Ly6E, Lymphocyte antigen 6 complex, locus E; mAb, monoclonal antibody; ADC, antibody-drug conjugate; SEC-HPLC, size exclusion column with high performance liquid chromatography

Figure 7. Biodistribution of radiolabeled anti-Ly6E ADC and -anti-Ly6E mAb in normal and tumor tissues following a single IV dosing of radiolabeled anti-Ly6E ADC or anti-Ly6E mAb; in tumor bearing mice. The graph is presented as %ID per gram of tissue of %ID per gram of blood. The solid bars represent the data by the non-residualized radioactivity of ^{125}I, while the hollow bars represent the data by the residualized radioactivity of ^{111}In. Data are represented as mean ± SD (N=5). **(A)** Distribution profiles at 1-day post dosing radiolabeled anti-Ly6E ADC or anti-Ly6E mAb where there was a significant reduced distribution to the tumor comparing the two molecules (* $p<0.01$); **(B)** Distribution profiles at 3-days post dosing radiolabeled anti-Ly6E ADC or anti-Ly6E mAb. Radioactivity in tumor for anti-Ly6E ADC was much more attenuated as compared to that of anti-Ly6E mAb, suggesting that the adduct formation resulted in a reduced internalization of ADC in tumor. (** $p<0.001$).

Ly6E, Lymphocyte antigen 6 complex, locus E; mAb, monoclonal antibody; ADC, antibody-drug conjugate; %ID, percent of injected dose; ^{125}I, iodine-125; ^{111}In, indium-111

DMD Fast Forward. Published on October 5, 2020 as DOI: 10.1124/dmd.120.000145
This article has not been copyedited and formatted. The final version may differ from this version.

Figure 8. In-vitro cell binding and uptake of radiolabeled anti-Ly6E ADC A1M adduct (preformed by pre-incubation with mouse plasma), -anti-Ly6E ADC control (no A1M adduct formation) and -anti-Ly6E mAb in tumor cell lines. HCC1937X1 (high Ly6E expression) and DOV13 (low Ly6E expression) cell lines were cultured and treated with the respective radiolabeled material as described in the "METHODS". **A)** Radioactivity levels in HCC1937X1 cell line as % of added radioactivity dose at 3h post-incubation. Data are represented as individual point ± SD (N=5); **B)** Radioactivity levels in DOV13 cell line as % of added radioactivity dose at 3h post-incubation. Data are represented as individual point ± SD (N=3). In both cell lines the comparison of cell binding and uptake of anti-Ly6E mAb to anti-Ly6E ADC without pre-incubation in plasma was not significant, however, the cell uptake for pre-formed A1M-ADC was significantly lower than the pre-incubated mAb ($p<0.01$).

Ly6E, Lymphocyte antigen 6 complex, locus E; mAb, monoclonal antibody; ADC, antibody-drug conjugate; A1M, alpha-1-microglobulin.

DMD Fast Forward. Published on October 5, 2020 as DOI: 10.1124/dmd.120.000145
This article has not been copyedited and formatted. The final version may differ from this version.

Tables

Table 1. Mean (± SD) Non-Compartmental PK parameters of anti-Ly6E mAb and anti-Ly6E ADC in C.B17 SCID mice and Sprague-Dawley rats.

SD, standard deviation; n, number of subjects; C_{max}, maximum concentration; AUC_{INF}, area under the concentration–time curve extrapolated to infinity; AUC_{Extrap_PRED}, percent of area under the concentration-time curve extrapolated from the last time point; CL, clearance; V_{ss}, volume of distribution at steady state; $t_{1/2}$, terminal half-life

Species	**Treatment dose, *N***	**C_{max}/Dose (µg/mL)/(mg/kg)**	**AUC_{INF} /Dose (day• µg/mL)/(mg /kg)**	**AUC_{Extrap_PRED} %**	**CL (mL/day/kg)**	**V_{ss} (mL/kg)**	**$t_{1/2}$ (day)**
Mouse[a]	anti-Ly6E mAb 1 mg/kg, n=3	24.0	244	36.6	4.12	85.6	14.6
Mouse[a]	anti-Ly6E ADC 1 mg/kg, n=3	26.1	300	31.4	3.33	59.7	11.7
Rat	anti-Ly6E mAb 5 mg/kg, n=4	25.2 ± 2.03	161 ± 63.2	14.7 ± 13.6	6.97 ± 2.60	79.6 ± 19.1	10.8 ± 5.94
Rat	anti-Ly6E ADC 2 mg/kg, n=5	28.2 ± 2.52	194 ± 84.3	22.0 ± 11.5	5.87 ± 1.88	68.5 ± 9.63	9.51 ± 4.02

[a] Parameters were calculated using naïve pooling approach

Table 2. Mean (± SD) Non-compartmental PK Parameters Cynomolgus Monkey anti-Ly6E ADC and Anti-Ly6E mAb

SD, standard deviation; n, number of subjects; C_{max}, maximum concentration; AUC_{inf}, area under the concentration–time curve extrapolated to infinity; AUC_{Extrap_PRED}, percent of area under the concentration-time curve extrapolated from the last time point; CL, clearance; V_{ss}, volume of distribution at steady state; $t_{1/2}$, terminal half-life

Treatment	**C_{max} (µg/mL)**	**C_{max}/Dose (kg•µg)/(mL/mg)**	**AUC_{INF} /Dose (day•µg/mL)/(mg /kg)**	**%AUC_{Extrap_PRED} %**	**CL (mL/day/kg)**	**V_{ss} (mL/kg)**	**$t_{1/2}$ (day)**
anti-Ly6E ADC (2 mg/kg, n=3)[a]	52.0 ± 12.2	26.0 ± 6.11	177 ± 35.7	16.0 ± 3.92	5.78 ± 1.10	61.3 ± 12.3	8.91 ± 0.907
anti-Ly6E ADC (4 mg/kg, n=6)[a]	98.3 ± 20.6	26.0 ± 3.58	205 ± 43.3	20.7 ± 8.04	6.82 ± 1.13	62.6 ± 5.46	7.25 ± 1.02
anti-Ly6E ADC (8 mg/kg, n=1)[a,b]	191	23.9	157	18.1	6.38	74.2	9.13
Anti-Ly6E mAb (0.3 mg/kg, n=2)[b]	9.31	31.0	222	7.92	4.51	71.2	11.9
Anti-Ly6E mAb	104 ± 11.7	34.6 ± 3.91	256 ± 14.0	7.53 ± 2.12	3.92 ± 0.221	60.2 ± 8.56	11.6 ± 1.18

(3 mg/kg, n=3)

[a] Parameters based on first cycle only

[b] Standard deviation (SD) was not calculated as n<3

DMD Fast Forward. Published on October 5, 2020 as DOI: 10.1124/dmd.120.000145
This article has not been copyedited and formatted. The final version may differ from this version.

DMD Fast Forward. Published on October 5, 2020 as DOI: 10.1124/dmd.120.000145
This article has not been copyedited and formatted. The final version may differ from this version.

Figure 1

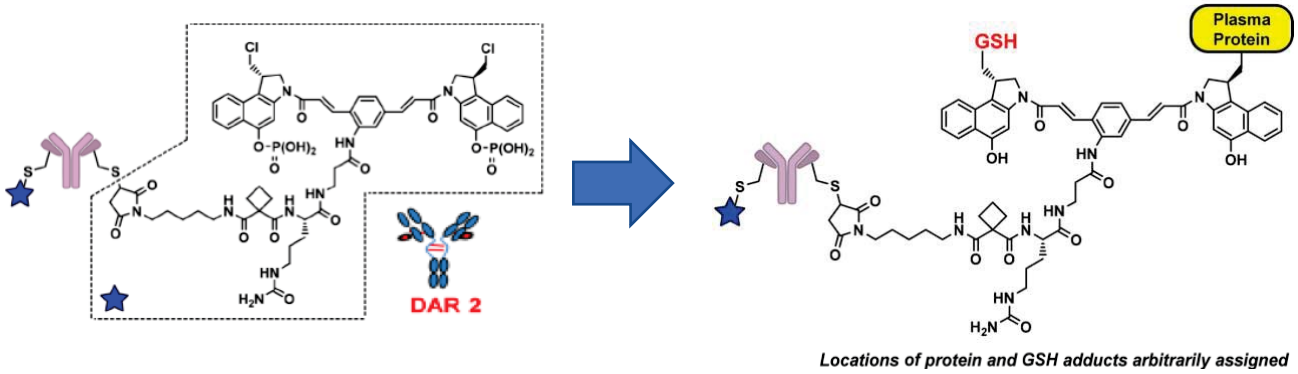

DMD Fast Forward. Published on October 5, 2020 as DOI: 10.1124/dmd.120.000145
This article has not been copyedited and formatted. The final version may differ from this version.

Figure 2

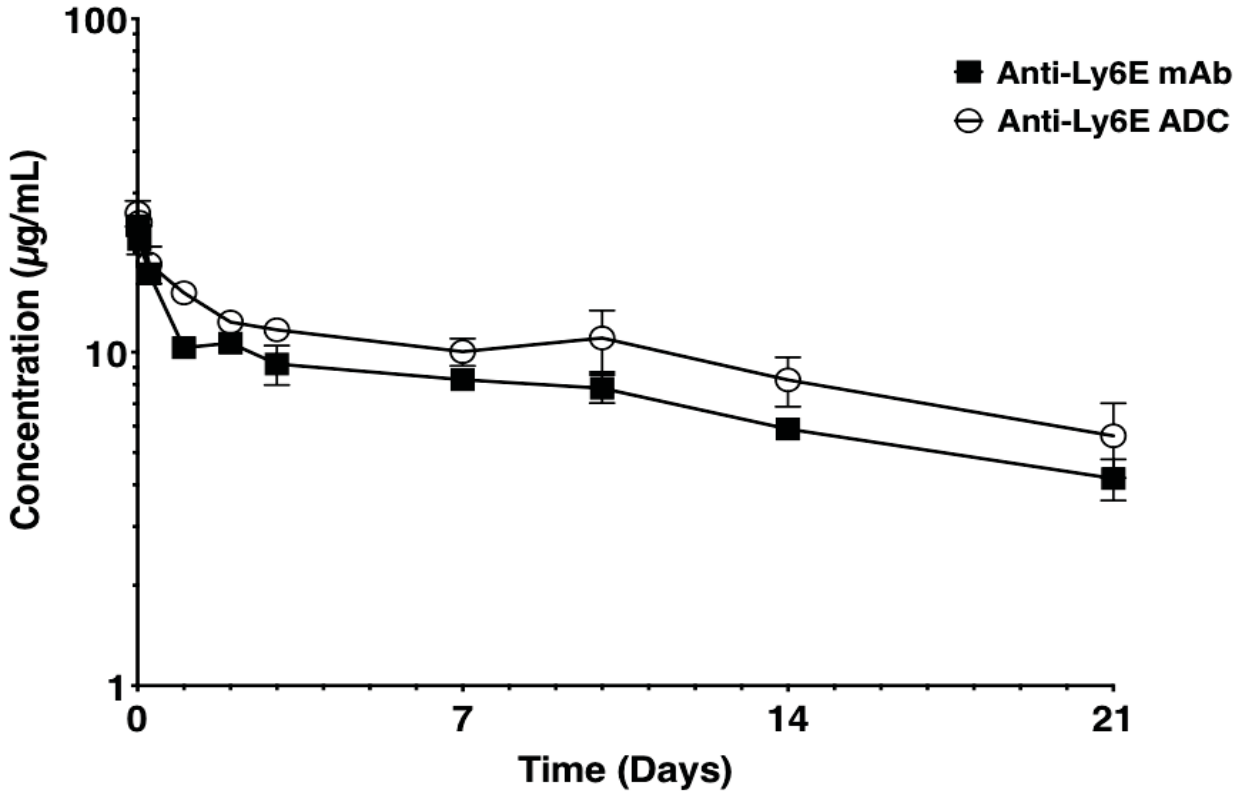

DMD Fast Forward. Published on October 5, 2020 as DOI: 10.1124/dmd.120.000145
This article has not been copyedited and formatted. The final version may differ from this version.

Figure 3

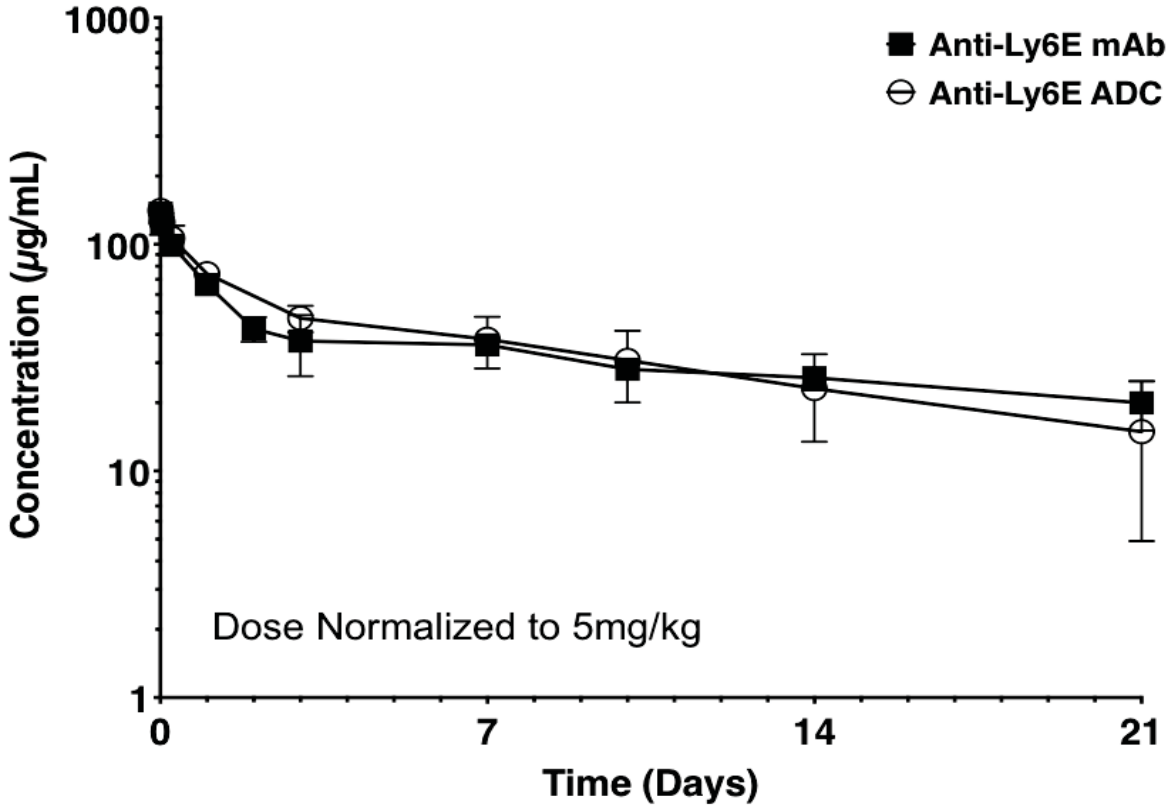

DMD Fast Forward. Published on October 5, 2020 as DOI: 10.1124/dmd.120.000145
This article has not been copyedited and formatted. The final version may differ from this version.

Figure 4

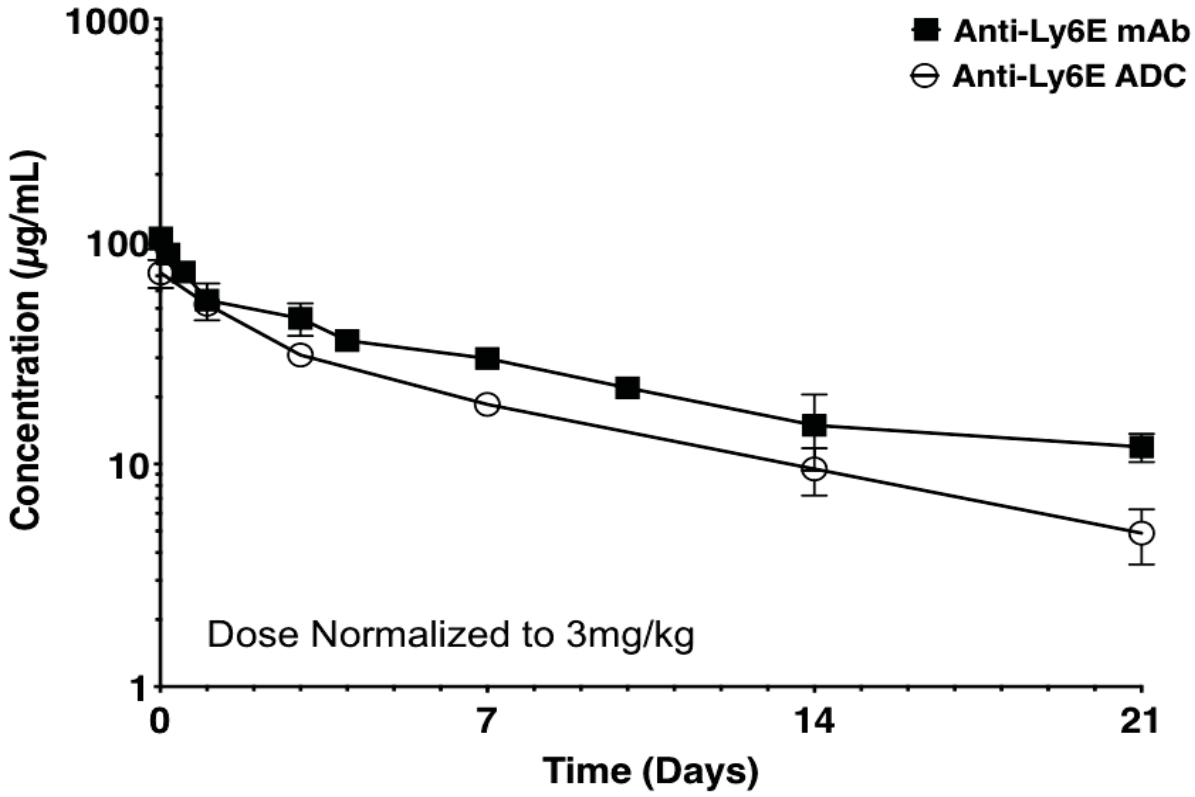

DMD Fast Forward. Published on October 5, 2020 as DOI: 10.1124/dmd.120.000145
This article has not been copyedited and formatted. The final version may differ from this version.

Figure 5

A

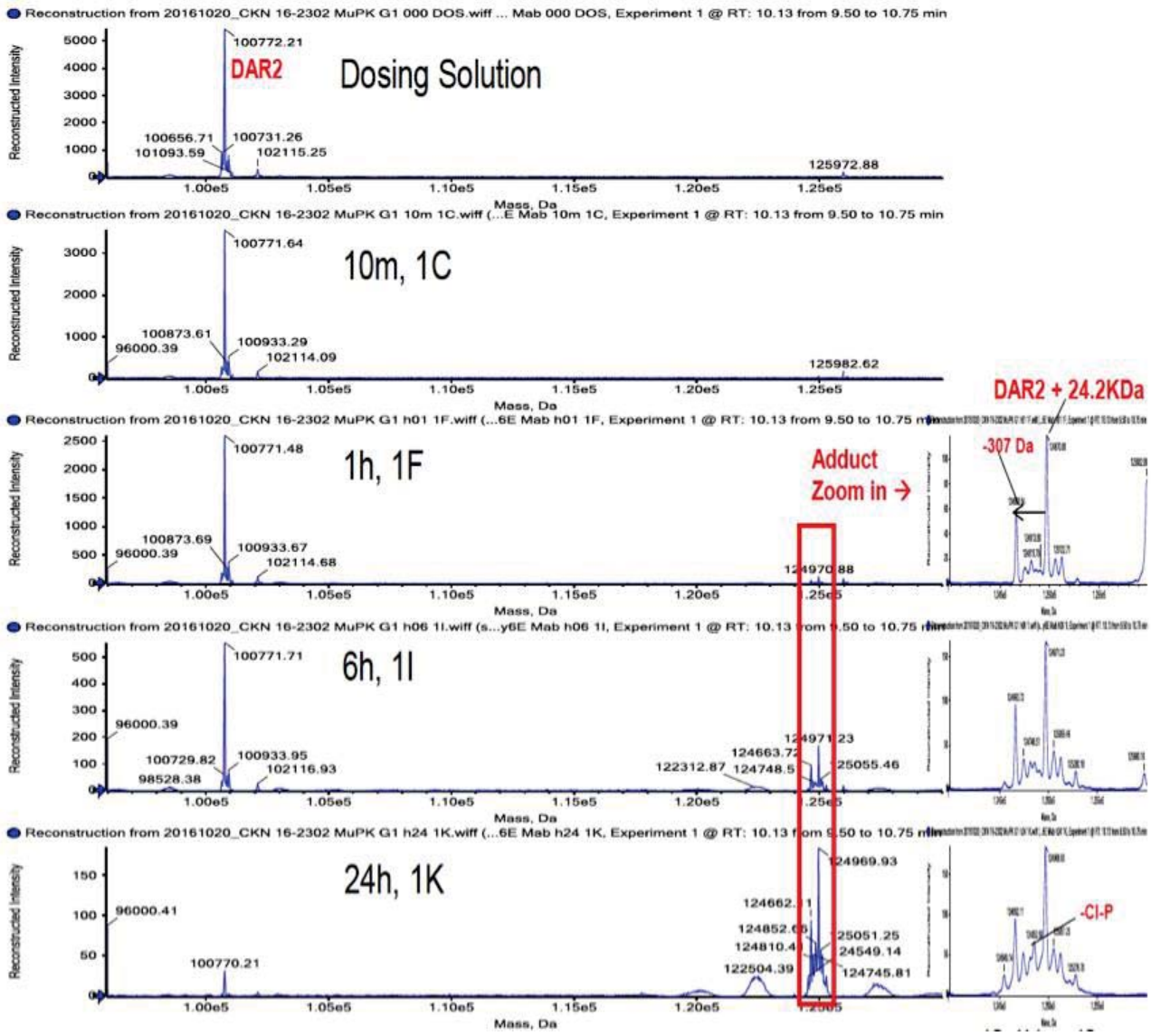

DMD Fast Forward. Published on October 5, 2020 as DOI: 10.1124/dmd.120.000145
This article has not been copyedited and formatted. The final version may differ from this version.

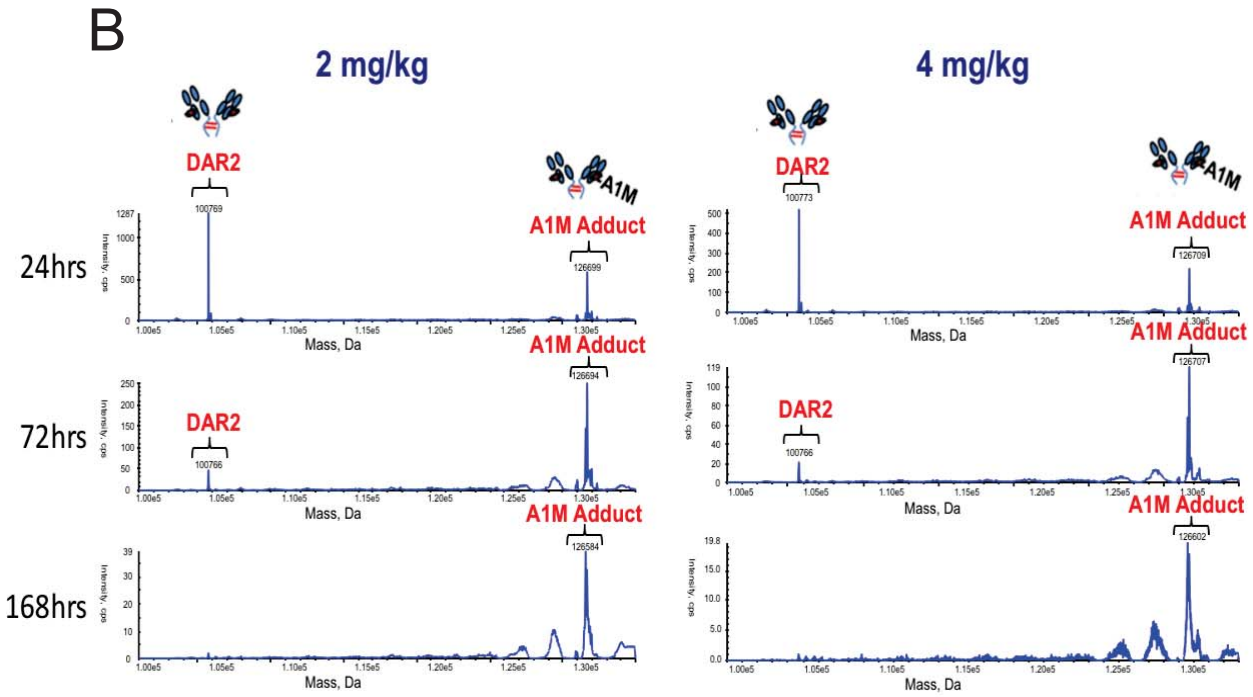

DMD Fast Forward. Published on October 5, 2020 as DOI: 10.1124/dmd.120.000145
This article has not been copyedited and formatted. The final version may differ from this version.

Figure 6

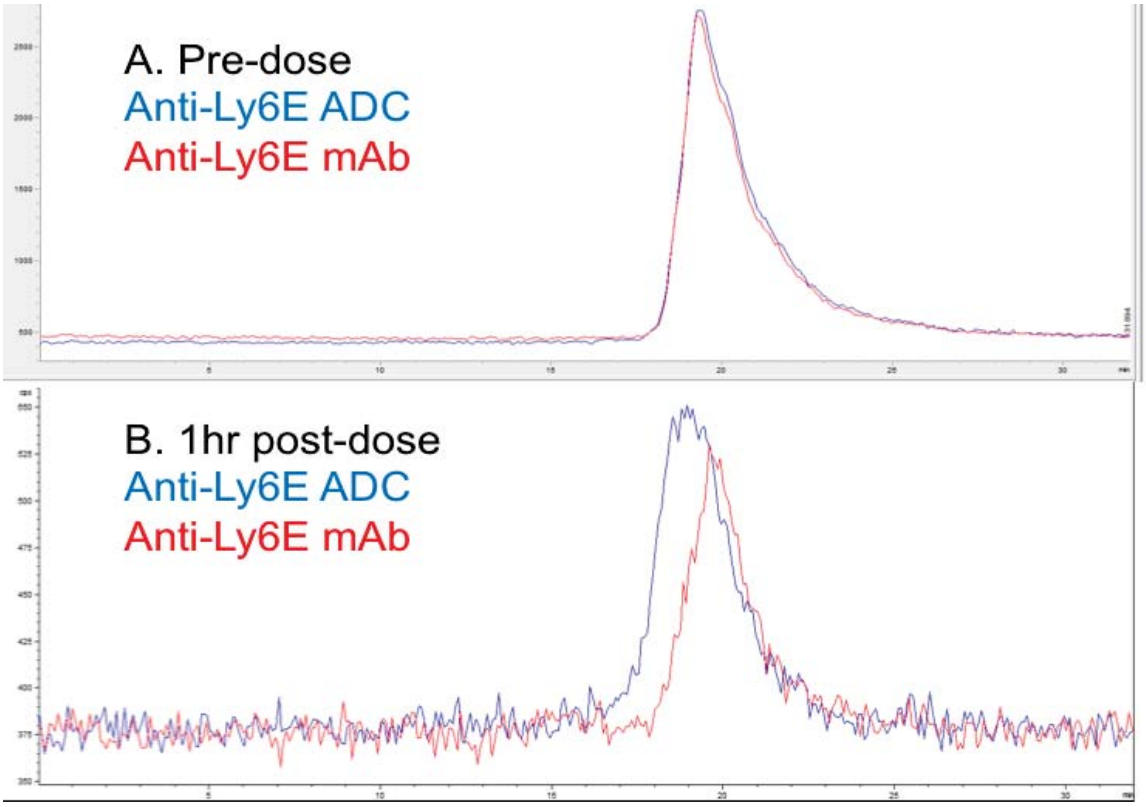

DMD Fast Forward. Published on October 5, 2020 as DOI: 10.1124/dmd.120.000145
This article has not been copyedited and formatted. The final version may differ from this version.

Figure 7

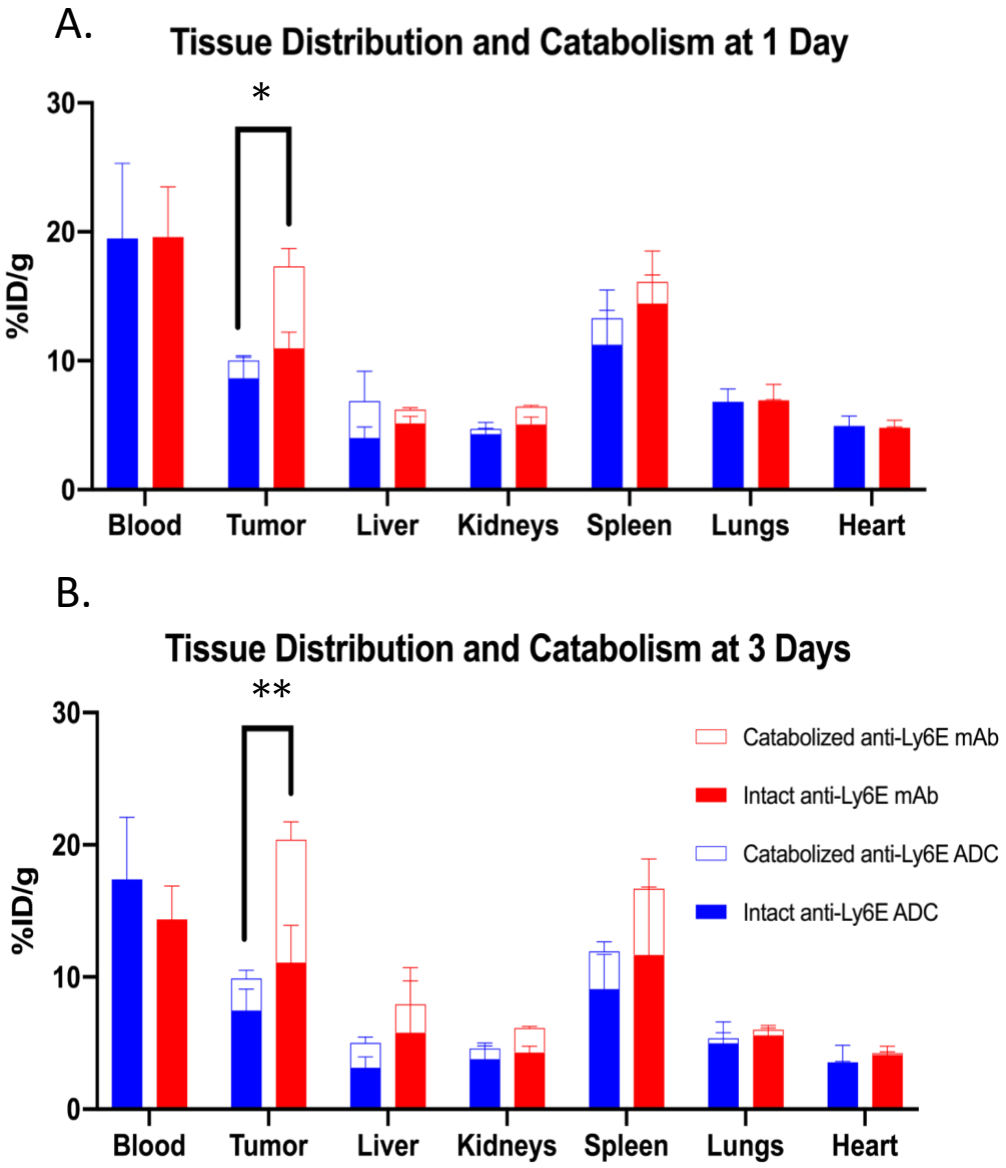

DMD Fast Forward. Published on October 5, 2020 as DOI: 10.1124/dmd.120.000145
This article has not been copyedited and formatted. The final version may differ from this version.

Figure 8

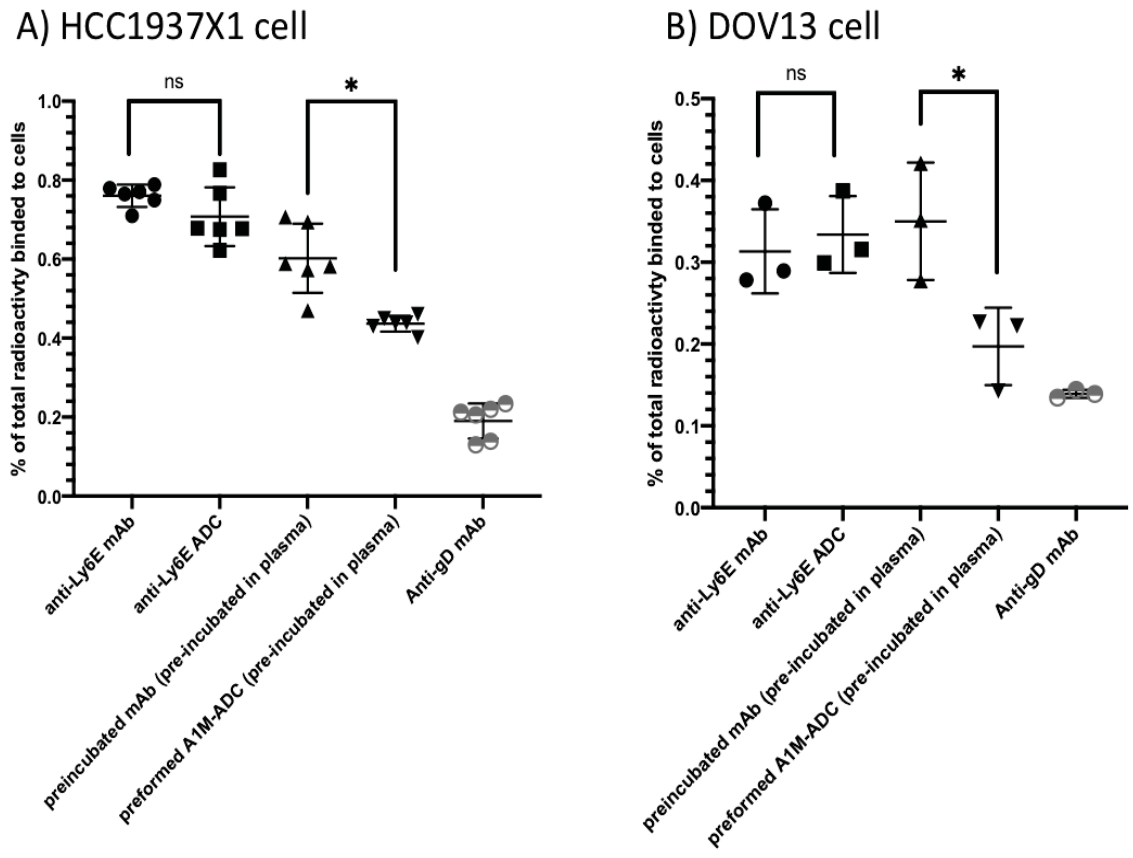

Supplementary Data

Anti-Ly6E-*seco*-CBI-Dimer Antibody-Drug Conjugate (ADC) That Forms Adduct with Alpha-1-microglobulin (A1M) Demonstrates Slower Systemic Antibody Clearance and Reduced Tumor Distribution in Animals

Victor Yip, Isabel Figueroa, Brandon Latifi, Shab Maish, Carl Ng, Doug Leipold, Amrita Kamath, and Ben-Quan Shen

Journal title: Drug Metabolism and Disposition

Manuscript number: DMD-AR-2020-000145

Supplementary Fig. 1

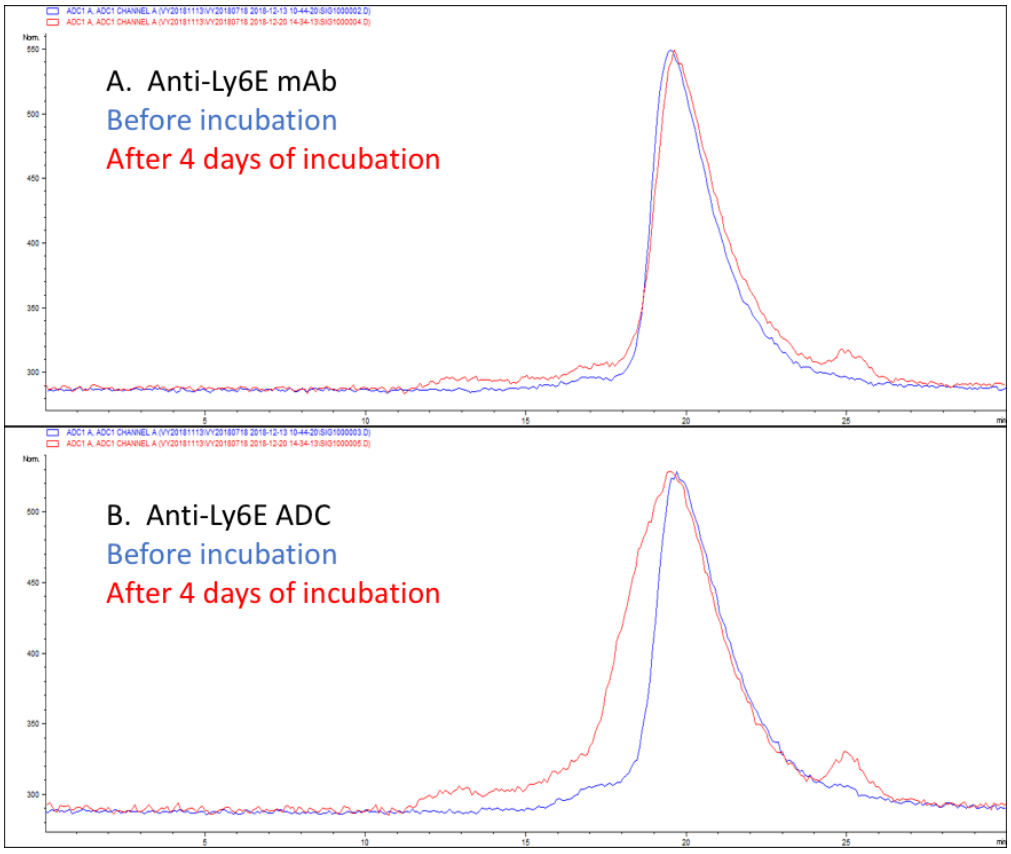

Supplementary Fig. 1. SEC-HPLC with in-line radio-detector chromatogram profile. **(A)** ^{125}I radiolabeled anti-Ly6E mAb before (blue) and after (red) in-vitro incubation in mouse plasma at 37^{o}C, have the same retention time where the two profiles overlapped. **(B)** ^{125}I radiolabeled anti-Ly6E ADC before (blue) and after (red) in-vitro incubation in mouse plasma at 37^{o}C, where ~50% of the radioactivity was left-shifted indicating the formation of A1M/protein adduct.

Supplementary Fig. 2

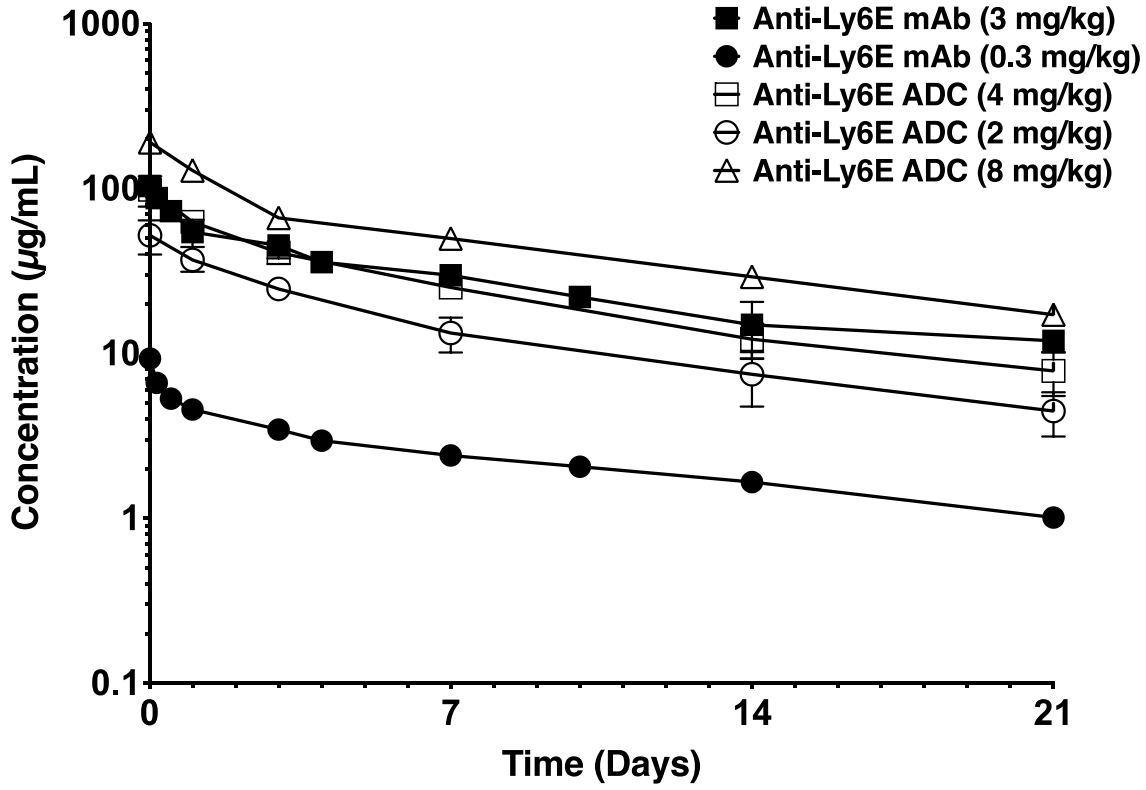

Supplementary Fig. 2. Mean (± SD) antibody concentration-time profiles of anti-Ly6E ADC (first cycle) following multiple IV doses (Q3w) and anti-Ly6E mAb following a single IV dosing in cynomolgus monkeys by individual dose group. Anti-Ly6E ADC was dosed at 2, 4, and 8mg/kg and anti-Ly6E mAb was dosed at 0.3 and 3 mg/kg (For

ADC, N=3, 6, and 1 for 2, 4, and 8 mg/kg respectively; For mAb, N=2 and 3 for 0.3 and 3 mg/kg, respectively).